JOURNAL OF AIRCRAFT
Vol. 45, No. 6, November–December 2008

Forced Separation and Reattachment of Flow to Glauert Laminar Airfoil Section II

Boris Zakharin* and Israel J. Wygnanski†
University of Arizona, Tucson, Arizona 85721

DOI: 10.2514/1.36027

The transient process of flow separation and reattachment to a concave surface was investigated experimentally on the rear ramp of a modified Glauert Laminar Airfoil Section II. The measurements were carried out at low incompressible speeds using miniature time-resolved piezoresistive pressure transducers (Endevco model). These measurements were supplemented by flow visualization and by exploratory use of a particle image velocimeter. It was observed that the concavity of the surface impeded flow reattachment, and therefore a much higher momentum coefficient was required to partially attach the flow to a concave surface than to a straight one when both surfaces were supposed to turn the flow by the same amount. Streamwise vortices were observed to exist on the concave ramp of the modified Glauert Laminar Airfoil Section II, and thus the interaction of streamwise and spanwise vortices and their impact on flow control are discussed. Lift augmentation by periodic excitation is mainly achieved by the entrainment of the upstream flow into the pulsating jet. For the on–off application of control, the transient time normalized by the time of flight between the actuator and the trailing edge varies between 15 and 20 over the upper and lower surfaces and between 5 to 15 over the ramp. The possibilities of gradually controlling the airfoil performance are also considered, and the phase delays of the surface-pressure perturbation are discussed.

Nomenclature

C_L	=	lift coefficient
C_p	=	pressure coefficient
$\langle C_p \rangle$	=	phase-averaged pressure coefficient
C_μ	=	steady momentum coefficient, $(2h/c)(U_{\text{slot}}/U)^2$
$\langle C_\mu \rangle$	=	oscillatory momentum coefficient, $(2h/c)\langle(U_{\text{slot}}/U)^2\rangle$
c	=	chord
F^+	=	nondimensional frequency, fL/U
f	=	frequency of excitation
h	=	slot width
L	=	characteristic length of the ramp
L_f	=	length of the flat flap
Re	=	Reynolds number, Uc/ν
t	=	time
U	=	freestream velocity
U_{slot}	=	jet velocity at the exit of the slot
x_s	=	slot x coordinate
α	=	angle of attack
δ_f	=	flap deflection angle
τ	=	nondimensional transient time, $tU/(c - x_s)$

I. Introduction

FLOW separation may be prevented or inhibited by fluidic intervention such as suction, blowing, or the periodic combination of the two that may, under a perfect balance, result in zero-mass-flux excitation [1–4]. The latter could be implemented by an actuation of a diaphragm that may not necessarily provide a simple harmonic motion [5]. Because periodic actuation is efficient and does not require central plumbing, extensive research was recently carried out on the subject. However, most of the published research articles focus on the end effect and the associated gadgetry that is required to achieve it, rather than on the understanding of the mechanism that prevents separation or leads to flow reattachment. In short, little is known about the transient that transforms the flow from a separated state to an attached state and vice versa. Such knowledge is required if one wants to use fluidic actuation to replace moving control surfaces that are slow, mechanically complex, and bulky.

II. Mechanisms of Unsteady Control

Detailed parametric studies that defined the optimal actuation required to maintain the flow attached or, alternately, that forces a separated flow to reattach were conducted on a generic flap configuration [6]. Large differences in the actuation level and/or its frequency that are necessary to achieve those two goals led to the conclusion that transition from a separated to an attached state requires a short burst of energy that might be relaxed after the final flow state was established. It means that the transition from a separated to an attached state and back involves a large hysteresis loop.

The transient separation and reattachment processes were only investigated on the generic flap configuration by using dynamically responsive pressure transducers on the surface considered, together with a particle image velocimeter (PIV) above it for mapping the flowfield [7,8]. It was realized that the reattachment process could be scaled with the time of flight of fluid particles over the flap, L_f/U, where U is the freestream velocity and L_f is the length of the flap, whenever the periodic actuation emanated from a slot located at the leading edge of the flap. Because the reattachment transient time was at least an order of magnitude larger than the typical excitation period, the reattachment process was independent of the initial phase of the impulsively initiated actuation. The flow reattached fastest when the reduced excitation frequency $F^+ \equiv fL_f/U \approx 1$. The control authority over the process was achieved by enhancing the large spanwise vortices dominating the flow through an increase in the oscillatory momentum input $\langle C_\mu \rangle$ and a change in the input frequency. Separated or idle fluid was transported away from the flap surface by a continuous array of eddies that were amplified spatially as they propagated over the flap. Spatial amplification of consecutive vortices resulted in a mean transport of fluid away from the flap surface, thus lowering the pressure over the surface and causing the main stream to reattach to it. The time required to separate the flow by ceasing the actuation was commensurate with the reattachment time.

Received 4 December 2007; revision received 28 May 2008; accepted for publication 30 May 2008.

*Research Assistant Professor, Department of Aerospace and Mechanical Engineering. Member AIAA.
†Professor, Department of Aerospace and Mechanical Engineering. Fellow AIAA.

Both processes could be slowed down substantially by slightly changing the input amplitudes instead of totally seizing or switching on the excitation.

The load on the flap surface does not decrease uniformly with the passage of time from the initiation of a controlled separation [6–8]. A cessation of the actuation or an abrupt decrease in the actuation frequency results in the formation of a large vortex above the flap that is akin to the dynamic-stall vortex seen often over rapidly pitching airfoils. This vortex temporarily increased the aerodynamic load over the flap before dropping it to its low separated value. The duration of this phenomenon decreased with increasing flap deflection. Abruptly increasing the frequency of the forced excitation from $F^+ < 3$ to ≈ 8 can also result in flow separation that does not generate a dynamic-stall vortex.

With the exception of a short initial period in which the reattachment process exhibits transient decrease in the normal-force coefficient [7], the load on the flap increases almost linearly with time during a forced reattachment of the flow. The duration of the initial adverse surge in flap loading is independent of the forcing frequency and is directly related to the initial vortex generated by the excitation. This vortex attaches the flow to the surface ahead (downstream) of itself, thus increasing the pressure downstream of the temporary reattachment location. The duration of the surge is determined by the convection speed of this vortex along the flap. Consequently, both the reattachment and separation processes are initiated by large vortices sweeping over the flap and generating forces that oppose the smooth transition from one state to the other.

The manipulation of the instantaneous forces and moments exerted by an aerodynamic control surface may require continuous changes in the imposed periodic excitation that entail switching between the separation and reattachment processes during their transient stages. An active flow control aileron would not have to move, provided that the adverse effects of such control could be eliminated. Preliminary experiments on the generic flap provided a proof of the concept by controlling flow separation through the use of high-frequency excitation. It turned out that the net force exerted by such an aileron was proportional to the duration of the induced separation before it was stopped or reversed [7].

The key feature sustaining attached flow at flap deflections exceeding the natural stall angles is the generation and artificial enhancement of large spanwise vortices. It was observed that the amplification of these vortices varies in space and in time during the forced reattachment. Close to the leading edge of the flap, the flow seems to be absolutely unstable during most of the reattachment process, enabling strong temporal amplification of some global modes. At the end of the process, the same region is only convectively unstable, permitting spatial amplification of the imposed excitation. This may also result in a very low initial advection speed of the large eddies.

One of the purposes of the current investigation is to extend the observations made on the generic flap to airfoils and, eventually, to finite wings as a precursor to closed-loop control strategies. A modified Glauert Laminar Airfoil Section II (GLAS II) was selected because its characteristics were thoroughly investigated in conjunction with steady suction, yet it embodies fluid-mechanical features for which the effects in turbulent flow are not well understood. Specifically, the flow over the rear portion of its upper loft [the ramp, as it is often referred to (see Fig. 1)], when forced to reattach, is centrifugally unstable and should contain quasi-stationary longitudinal vortices that interact and distort the mean flow, in addition to the large Kelvin–Helmholtz (K–H) eddies that are enhanced by periodic excitation. A schematic view of such interaction is shown in Fig. 2. It focuses on the distortion of the K–H modes by the Gortler (G)-type eddies. The process resembles the bending of the large spanwise vortices in a turbulent mixing layer emanating from a chevron trailing edge [9]. It is not known whether centrifugal instability helps to keep the flow attached to the surface or impedes it, as is probably the case of a wall jet flowing over a convex surface (the Coanda effect), and the longitudinal eddies may be the ultimate cause of flow separation. In the case of the wall jet, the behavior of the longitudinal vortices (G-type) is reasonably well

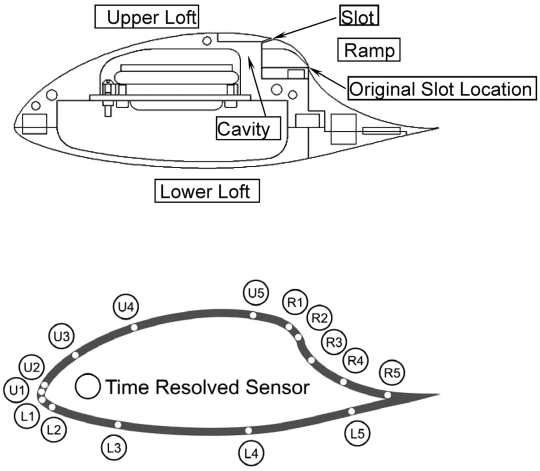

Fig. 1 Schematics and the pressure-tap locations for the Endevco on the modified GLAS II airfoil.

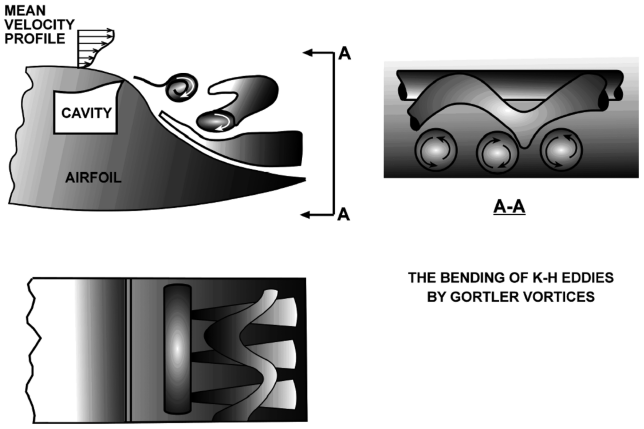

Fig. 2 Sketch of the large eddies generated over the ramp of the GLAS II airfoil.

understood [10,11] and the interaction between K–H and G-type eddies was at least proven to exist [12].

There has been a considerable interest in the flow over a hump that was placed on the wall of a wind tunnel. The shape of the hump represented the ramp of a GLAS II airfoil [13,14]. Active flow control was also used in this experimental investigation that became a benchmark for computational fluid dynamics (CFD) code validation. The differences between the flow over such a hump and the flow over an airfoil are not trivial, because in the latter case, there is a change in the circulation that strongly affects the boundary-layer characteristics over the upper surface. These differences should be fully understood and properly documented.

The present investigation describes first the aerodynamic qualities of the airfoil with and without active separation control at $Re < 0.5 \times 10^6$. The flow over the airfoil and, in particular, over its rear ramp was then probed under steady conditions before embarking on the transients associated with separation and reattachment. The values of the control parameters $\langle C_\mu \rangle$ and F^+, which were selected for the experiments, are by no means entirely representative of all physical situations possible, nor do they represent all the control schemes available. However, sufficiently meaningful results were accumulated to warrant the sharing of the information.

III. GLAS II Airfoil

The GLAS II airfoil (Fig. 1) has a maximum thickness-to-chord ratio of 31.4% and was originally designed to operate with massive suction through a slot located at 69% of the chord [15]. The designer intended to have favorable pressure gradients over most of the upper

and lower lofts, thus maintaining laminar flow over a large fraction of the airfoil surface. The large thickness of the airfoil and its asymmetry permit the generation of substantial C_L without the use of flaps. Suction provided a pressure discontinuity across the slot that led to a positive pressure along the aft of the concave ramp. With adequate suction [16], the measured L/D varied from 250 to 550 for $C_L > 1$ and $Re \approx 10^6$, provided that the surface of the airfoil was smooth. In the absence of suction, there is a major deterioration in the aerodynamic performance of the airfoil that provides $L/D \approx 12$ at $C_L \approx 0.6$ at the same Reynolds number. The L/D increased to approximately 30 at $Re \approx 3 \times 10^6$. Surprisingly, it appeared that the flow was intermittently reattaching to the ramp just upstream of the trailing edge, resulting in large drag oscillations. Blowing appeared to be less effective than suction, requiring a larger mass flux to forcibly reattach the flow [15]. Either way, the C_μ required to keep the flow attached was excessive. Many additional research papers followed, tests were carried out under high pressure [17] to obtain large Reynolds numbers, a trailing-edge flap was added [18], and the GLAS II wing was tested in flight on a glider [19]. If comparable performance improvement could be achieved using periodic excitation at considerably smaller $\langle C_\mu \rangle$ levels, the interest in GLAS II-type airfoils could be revived. The large volume inside the airfoil, which may be used for transport of cargo, makes GLAS II a good candidate for a span loader or a joint-wing concept. The rich interacting fundamental flow phenomena stimulated by the airfoil's shape make it very attractive for research.

IV. Experimental Setup and Data Acquisition

The GLAS II airfoil used in the present experiment had a chord length of 9.91 in. The original slot location was modified from the 69% of the chord suggested by Glauert [15], to 62%, as used in later references [5,19,20]. The actuation location was moved upstream because the intended low level of actuation was unable to affect the flow at small angles of incidence at the original slot location. The Australian researchers faced similar difficulties and they, too, moved the suction location [19] upstream and slightly altered the geometry near the slot. The chosen 62%-chord location of the slot corresponds to the separation line predicted by Hassan[‡] using NASA's CFL3D program [21] that accounted for the normal pressure gradient across the boundary layer and was modified to enable its use in conjunction with active flow control. The CFD predictions for the location of separation, and hence for the assigned slot location, were confirmed by the experiments.

Seven internal actuators situated in a sealed chamber in the airfoil's interior generated the periodic flow perturbations. The oscillatory flow passed through a contoured contraction to the slot, resulting in an oscillatory blowing jet with zero net mass flux at its origin. A signal generator was used to supply the desired voltage variation to the actuators. The amplitudes of the slot excitation were determined for each input voltage and frequency by a single hot-wire probe located at the slot exit during a calibration procedure. The results were used to calculate an oscillatory momentum coefficient $\langle C_\mu \rangle$.

For the clean airfoil, there is a strong hysteresis in C_L between $\alpha = 0$ and 8 deg; namely, different values of C_L are obtained for the same angle of attack, depending on whether α was decreased or increased [22]. The hysteresis was attributed to the formation of a separation bubble on the upper surface downstream of $x/c = 0.4$. To prevent the separation at that location, a 60-grit equivalent-sand-roughness strip was glued to the surface at 36% of the chord in some of the experiments. The flow downstream of the strip became turbulent, resulting in the disappearance of the bubble. The 60-grit roughness was experimentally found to cause transition in the range of Reynolds numbers considered.

The china-clay technique was used to visualize the flow above the upper surface of the wing. Because the airfoil was installed vertically in the wind tunnel, a thin horizontal partition matching the shape of the upper surface was attached to it horizontally.

[‡]Private communication with A. Hassan.

The visualization of the vortices by light-sheet and PIV measurements were performed in the crossflow plane over the ramp. A dual-pulsed laser sheet illuminated the plane perpendicular to the flow over the ramp spanning the entire wind-tunnel width. A charge-coupled-device camera synchronized to the laser was used to take one picture per laser pulse, resolving the movement of the seeding particles between two successive frames as taken by the camera. A commercially available smoke generator produced the seeding particles (smoke).

The airfoil was equipped with 56 static pressure ports, 15 of which were connected to high-frequency response (Endevco model 8507C-1) pressure transducers. They were divided into three groups. Those located upstream of the slot were labeled by the letter U, those on the ramp were labeled by R and those on the lower surface were labeled by L. They were distributed unevenly along the center span, as shown in Fig. 1. In addition, one unsteady transducer was installed in the slot for monitoring the actuators and providing a synchronization signal. All unsteady pressures were acquired simultaneously at a sampling rate of 2048 Hz per transducer. The resolution of the pressure transducers was approximately 1 Pa, and the anticipated error in the calculated pressure coefficients is of the order of 1%. The airfoil was mounted vertically in the 3 by 4 ft Skobie wind tunnel located at the Aerospace and Mechanical Engineering Department of the University of Arizona at speeds $U < 40$ m/s, corresponding to Reynolds numbers, based on the airfoil chord, of $Re < 0.5 \times 10^6$.

V. Flow Visualization and Preliminary Consideration

Flow visualization using china clay brushed on a horizontal plane normal to the upper surface of the airfoil reveals the streamline pattern above the airfoil (Fig. 3). In the absence of actuation, the flow separates from the surface near the slot and remains separated over the ramp (Fig. 3a). Because the flow leaves the surface at a direction that is tangential to the upper loft at separation, a large dead-air zone is present downstream of the slot. The jet created by periodic excitation vigorously entrains the ambient fluid above it, causing the streamlines to bend and become almost normal to its mean trajectory near the slot (Fig. 3b). The increase in the curvature of the streamlines above the airfoil's upper loft is an indicator of the low pressure that had been generated by the periodic excitation (Fig. 3b). Such a low-pressure region upstream of the jet exit (Fig. 4) is strongest near the

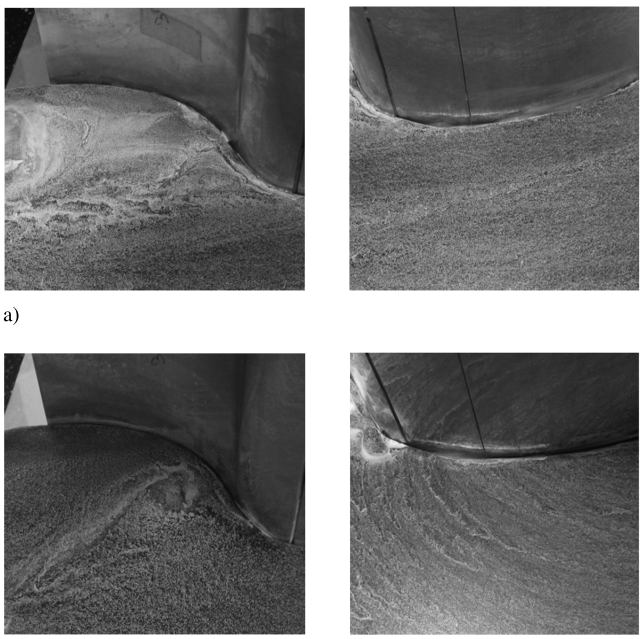

a)

b)

Fig. 3 Clean airfoil at $\alpha = 6$ deg, 7 m/s, and $Re = 1.13 \times 10^5$: a) baseline and b) AFC $F^+ = 2.88$ (200 Hz) and $\langle C_\mu \rangle = 10\%$; regions of the ramp and the upper loft are shown.

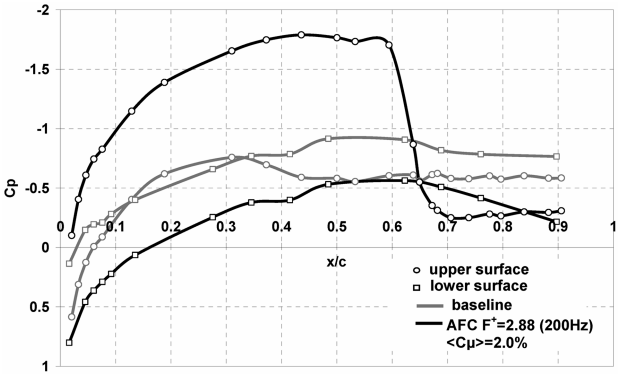

Fig. 4 Mean pressure distribution over the clean airfoil at $\alpha = 6$ deg, 7 m/s, and $Re = 1.13 \times 10^5$: a) baseline, b) AFC $F^+ = 2.88$ (200 Hz) and $\langle C_\mu \rangle = 2\%$.

nozzle and decreases in the direction of streaming. The upstream curvature of the entrained streamlines is dependent on the level of the actuation and it was also observed at much lower levels. The outer boundary of the mixing layer is clearly observed in Fig. 3b, in which the preferred location of the first rollup of the large eddies in this mixing layer can also be detected.

The shear layer created between the outer stream and the dead-air zone is bent toward the surface instead of proceeding straight in the direction of the freestream (Fig. 3b), due to the asymmetrical entrainment of the ambient air that is most prominent at the beginning of the actuation on the low-velocity side of the mixing layer. This entrainment bends the mixing layer toward the surface because the amount of fluid residing between the surface and the high-speed stream is limited; thus, the fluid removed from this region reduces the pressure within it, forcing the flow to bend toward the surface, until an equilibrium between pressure difference and centrifugal force is attained. In general, the entrainment is intensified by steadily injecting high-speed flow (blowing) or by increasing the amplitude of the periodic actuation.

In the case of a *convex* upper loft of an airfoil, the equilibrium between pressure and centrifugal forces across the mean streamlines may be maintained until its trailing edge, but this is not the case on the GLAS II airfoil, on which the curvature changes sign along the ramp. In the absence of strong mixing, the low-pressure zone should have switched from the surface to the freestream in which the curvature changed sign. It did not do that because of the rapid divergence of the streamlines. This implies that the mixing layer, created by periodic actuation, diverges strongly in the direction of streaming and decelerates due to the entrainment, rather than due to the adverse pressure gradient. Such entrainment might have been enhanced by the existence of longitudinal vortices created by centrifugal instability of the mixing layer (or a boundary layer that is continuously on the verge of separation) [23]. As a consequence, the momentum input required to attach the flow to a *concave surface* is significantly higher than that to a convex surface and the result is, more often than not, incomplete. For example, to attach the flow over a 25%-chord flap that is deflected at 40 deg to the chord of a NACA 0015 airfoil requires $\langle C_\mu \rangle$ of the order of 1% [24], whereas an order of magnitude higher $\langle C_\mu \rangle$ is required to *partly* attach the flow to the surface of the ramp on the GLAS II airfoil.

The immense difference between the momenta required to turn the outer flow by a similar angle in these two cases may be considered from two points of view: the hypothetically attached flow and the separated flow. In the first case, the concave-ramp surface that is downstream of a convex transitional portion of the airfoil generates an adverse pressure gradient seen by the approaching boundary layer. It is partly due to the thinning of the airfoil, resulting in the divergence of the streamlines, and partly due to the change in the sign of the streamline curvature, as discussed previously. Only very strong tangential blowing will change the shape of the velocity profile over the ramp by turning the boundary layer into a wall jet and making it stable in the centrifugal (Görtler) sense. Strong blowing is therefore able to withstand the adverse pressure gradient without separating. When the crossflow pressure gradient is appreciable, the boundary-layer concept, as we know it, breaks down. The tremendous rate of spread of the jet that entrains most of its added fluid from the far field (e.g., Fig. 3b) is a clear testimony to these effects.

In the initially separated flow case, the free mixing layer becomes convex in response to the fluidic intervention that lowers the pressure between it and the surface. Increasing the input amplitude or momentum of that intervention will tend to increase the convexity of this shear layer, which may be opposed by the concave surface in its vicinity, breaking it into an array of bubbles that trail each passing vortex created by Kelvin–Helmholtz instability. In this case, the local curvature of the streamlines changes periodically with time, thus avoiding the constant requirement that the highest pressure will occur over the surface. This is possibly the reason why the reattachment to a concave surface requires very high control amplitude, and even then, such reattachment may be periodic (Fig. 3b). One may also argue that applying active flow control to a separated flow over a concave surface requires a larger value of $\langle C_\mu \rangle$, because the volume of the fluid between the separating streamline and the receding surface is larger than in the corresponding convex case.

The convex curvature of the entrained streamlines reduces the pressure on the surface upstream of the slot, and this curvature increases the lift on the GLAS II even when the flow farther downstream separates. If the separated jet trajectory is approximately straight, then the mean surface pressure along the ramp should be approximately constant.

The effects of the high-amplitude excitation on the ensuing mixing layer are visible in Fig. 3b. At $\langle C_\mu \rangle = 10\%$, the first rollup of the shear layer occurs around $x/c = 0.75$. The rolled-up vortex is so strong that the mixing layer bends toward the surface and the flow seemed to enclose a small bubble upstream of the rollup location. Farther downstream, the jet spreads out so quickly that its width is commensurate with the maximum thickness of the airfoil in the vicinity of the trailing edge. For the weaker $\langle C_\mu \rangle = 2\%$, the first rollup occurs farther downstream (opposite $x/c = 0.9$, not shown) and it is not as big and as clearly defined as it is for the larger $\langle C_\mu \rangle$. The change in the curvature of the entrained streamlines in this case occurs much closer to the slot and it is not as severe as for the higher values of $\langle C_\mu \rangle$. Nevertheless, there is a rapid deceleration of the flow over the ramp that manifests itself in an increase in C_p. The increase in C_p of approximately 1.5 was observed between $0.6 < x/c < 0.67$ (Fig. 4), which resulted in an increase in the trailing-edge base pressure of $\Delta C_p = 0.5$ relative to the baseline case. Nevertheless, the C_p at the trailing edge was still somewhat negative, suggesting that complete flow attachment was not attained.

The streamwise (Görtler) vortices generated on the concave-ramp surface due to the centrifugal instability were visualized by a laser light sheet in the crossflow plane of the ramp and the results are shown in Fig. 5. The counter-rotating vortices are clearly identified. Note that when the excitation is applied, the vortices approach the ramp surface. Photographs of the flow velocity in the crossflow plane were measured by PIV, and preliminary vorticity contours ensemble-averaged over 100 events are shown in Fig. 6. Periodic

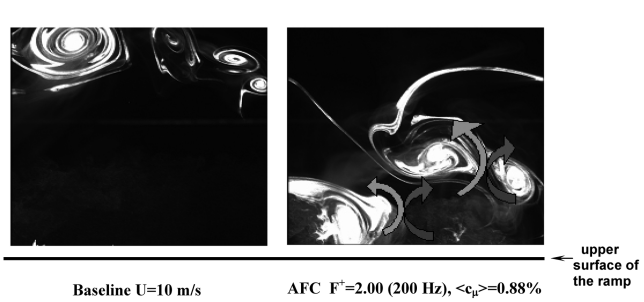

Fig. 5 Light-sheet visualization in the crossflow plane over the ramp at $x/c = 0.8$ and $Re = 1.61 \times 10^5$ with the boundary layer tripped.

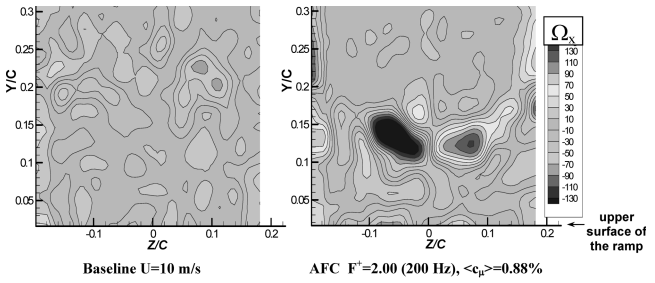

Fig. 6 Ensemble-averaged PIV image of streamwise vorticity distribution over the ramp at $x/c = 0.8$ and $Re = 1.61 \times 10^5$ with the boundary layer tripped.

excitation even at the low level of $\langle C_\mu \rangle = 0.88\%$ enhanced the ensemble-averaged contours of these streamwise vortices and brought them closer to the surface.

VI. Controlled Transients of Flow Reattachment and Separation

A good understanding of the transients is important whenever fluidic actuation is to be used for control, because knowing the flow response to changes in forcing parameters is necessary for the construction of a functional controller. The condition of the flow over a generic flat flap [6] at moderately high Reynolds depends on three parameters: flap deflection angle δ_f, $\langle C_\mu \rangle$, and F^+. These parameters regulate the switch between separated and attached states, but due to the hysteresis of the transition, an existing state of the flow depends not only on its initial state [6], but also on the path that was taken to change that state (i.e., whether the amplitude was altered at a given F^+ or the frequency was changed at a given amplitude). Although an infinite number of paths and arbitrary time dependence on $\langle C_\mu \rangle$ and on F^+ are possible, only step changes in these parameters were considered in previous investigations [6–8], because they revealed the most pronounced changes occurring in the flow. The same approach was presently adopted as being a prerequisite for a closed-loop control scheme, and other control paths may be considered in the future.

A. Forced Reattachment

Consider the attachment of separated flow to the upper surface of a clean airfoil (in the absence of boundary-layer tripping strips) in response to a sudden application of periodic excitation. Time-resolved static pressures that were phase-locked to the forcing signal were measured during such a reattachment process. These time-varying pressures, containing the oscillating component of the excitation frequency, were locked to the initiation of the excitation that always started at the same phase of the forcing signal. The experiment was repeated approximately 30 times and the data were ensemble-averaged. Typical variations of C_p with time at the indicated locations on the airfoil are shown in Fig. 7, together with the mean static pressure distributions measured before and after a partial reattachment of the flow. The data were taken at an incidence of $\alpha = 6$ deg and $Re = 2.26 \times 10^5$ at an optimal excitation frequency of $F^+ = 1.44$ and a considerably large final amplitude of $\langle C_\mu \rangle = 2.5\%$. The large lift generated by the forced reattachment

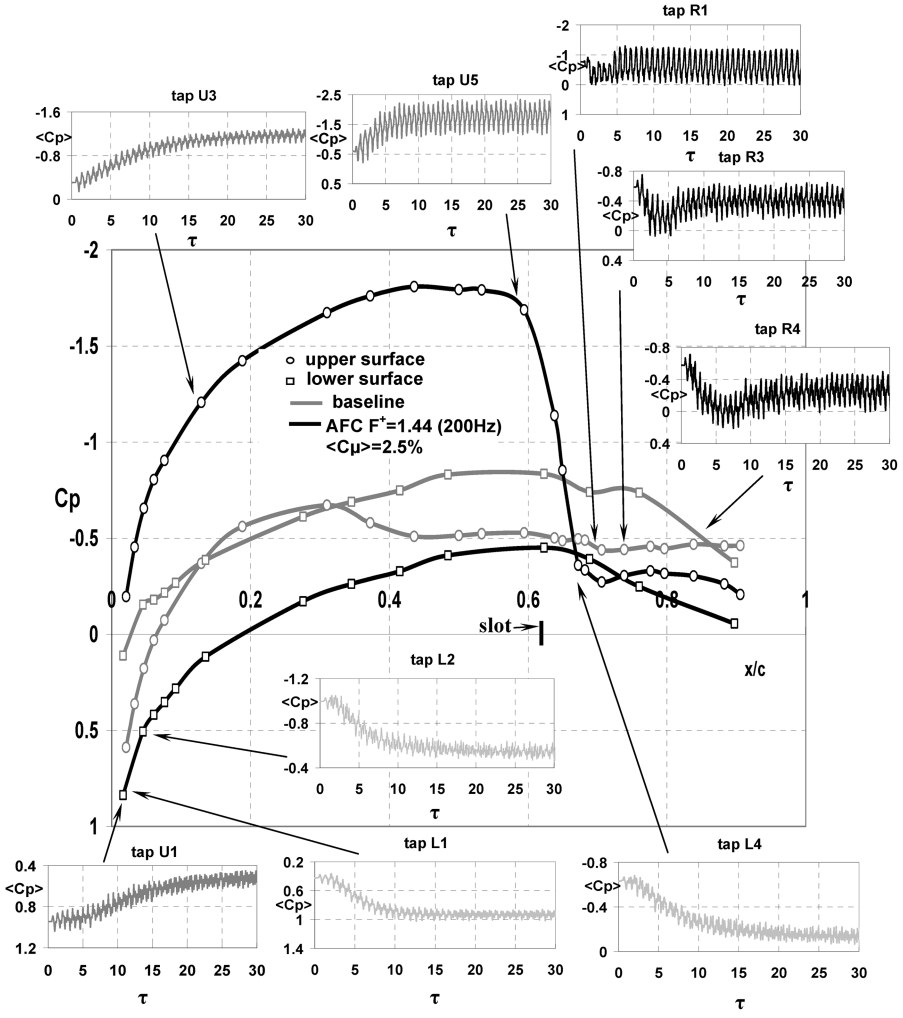

Fig. 7 Mean C_p for separated and attached flow and transient pressure signatures during reattachment on a clean airfoil at $\alpha = 6$ deg and $Re = 2.26 \times 10^5$ ($U = 14$ m/s).

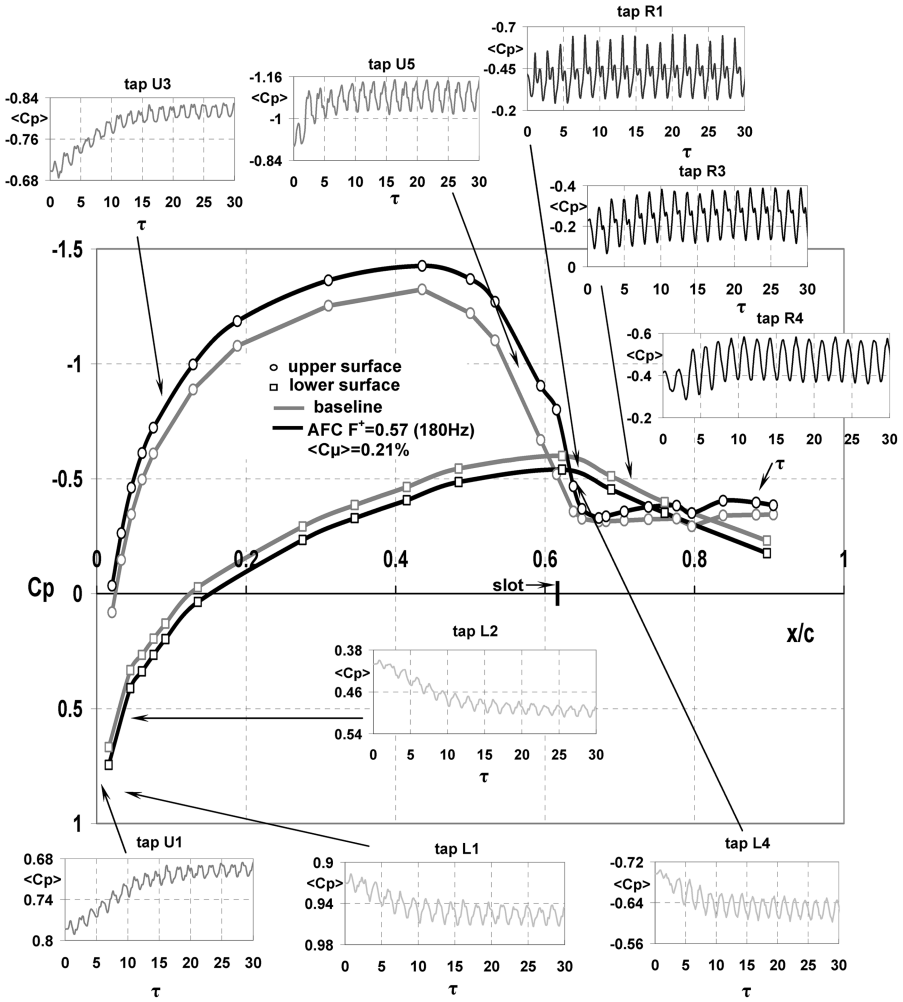

Fig. 8 Mean C_p for separated and attached flow, and transient pressure signatures during reattachment on the airfoil with a tripped boundary layer at $\alpha = 8$ deg and $Re = 4.84 \times 10^5$ ($U = 30$ m/s).

is obvious by simply comparing the two mean C_p distributions. Most of the increase in lift is attributed to changes occurring upstream of the slot, although some reattachment of the flow can be deduced from the downstream pressure changes as well.

The two fundamental time scales associated with the reattachment (i.e., the period of the excitation and the time necessary for completing the process) resemble the time scales observed on the generic flap [7]. The dimensionless transient time required for the flow to reattach, $\tau = tU/(c - x_s)$, varies between $5 < \tau < 20$, where $\tau = 5$ occurs on the ramp, and values of $\tau > 10$ were measured elsewhere on the airfoil. The distance $(c - x_s)$ represents the projected straight distance between the slot and the trailing edge along the airfoil's chord, and it is approximately equal to the characteristic length L of the ramp. Tripping the boundary layer on this airfoil, changing the Reynolds number, incidence, and even reducing the $\langle C_\mu \rangle$ by an order of magnitude had no substantial effect on τ. The transient times elapsing between the two steady-state conditions did not change, even when the degree of the added momentum was minimal ($\langle C_\mu \rangle = 0.21\%$) and the flow over the airfoil was tripped (Fig. 8). Because the baseline flow in the second example (Fig. 8) was mostly attached, the differences in the mean values of C_p resulting from the actuation are small (note the different scales in the insets), as is the change in the lift generated. Relatively significant C_p modification happened on the convex part of the ramp due to the reattachment (Coanda effect). The transient changes in the pressure distributions over the ramp shown in Fig. 7 do not vary monotonically with time. This peculiar variation was attributed to an initial creation of a large bubble for which the size diminished with time; it could be eliminated altogether by tripping the upstream flow.

The actuation disturbance propagates to all regions of the airfoil at the velocity of sound. This propagation of the disturbance is therefore independent of Reynolds number and of the condition of the boundary layer (i.e., whether it was tripped or not). On the ramp, however, the disturbance is dominated by vortices created by the shear waves, which propagate with local convective velocity that is related to the freestream.

The phase differences between the signatures of pressure transducers located on the upper surface, excluding the ramp, are difficult to assess, partly because of the high speed of the disturbance propagation and partly because of the complex shape of the pressure signal and the relatively low-frequency response of the transducers. Nevertheless, when the distance between transducers on the upper surface exceeded 15 cm, the estimated phase difference yielded a velocity that was approximately equal to the velocity of sound, as shown in Fig. 9. It is interesting to note that the waveform at the higher frequency of excitation is purer than at the lower frequencies. Because the experiment was repeated at frequencies ranging from 100 to 400 Hz (Fig. 10a), it became obvious that the transient time is independent of the excitation frequency. When the signal was low-pass-filtered at 50 Hz and normalized, as shown in Fig. 10b, it appeared that the transient process of reattachment was completed at $\tau \sim 20$, being insensitive to the frequency of the excitation. The total transient time measured from the beginning of the pressure drop was approximately $\Delta\tau \sim 15$ (Fig. 10b).

In the ramp region, the situation is different. Expanded pressure signatures over the ramp in the absence of tripping, showing the transient process of reattachment with a final $\langle C_\mu \rangle$ of 2.5% at $F^+ = 1.44$, are plotted in Fig. 11. In this case, no phase lags were

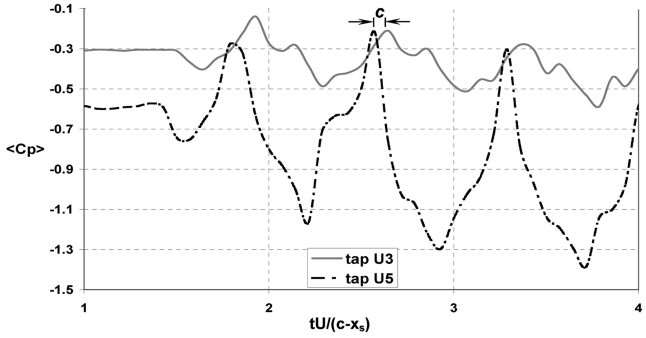

Fig. 9 Pressure signatures on the upper surface during the initial stage of reattachment on a clean airfoil at $\alpha = 6\,\text{deg}$, $Re = 2.26 \times 10^5$ (14 m/s), AFC $F^+ = 1.44$ (200 Hz), and $\langle C_\mu \rangle = 2.5\%$ (25 V); length c corresponds to the phase shift of the sound wave.

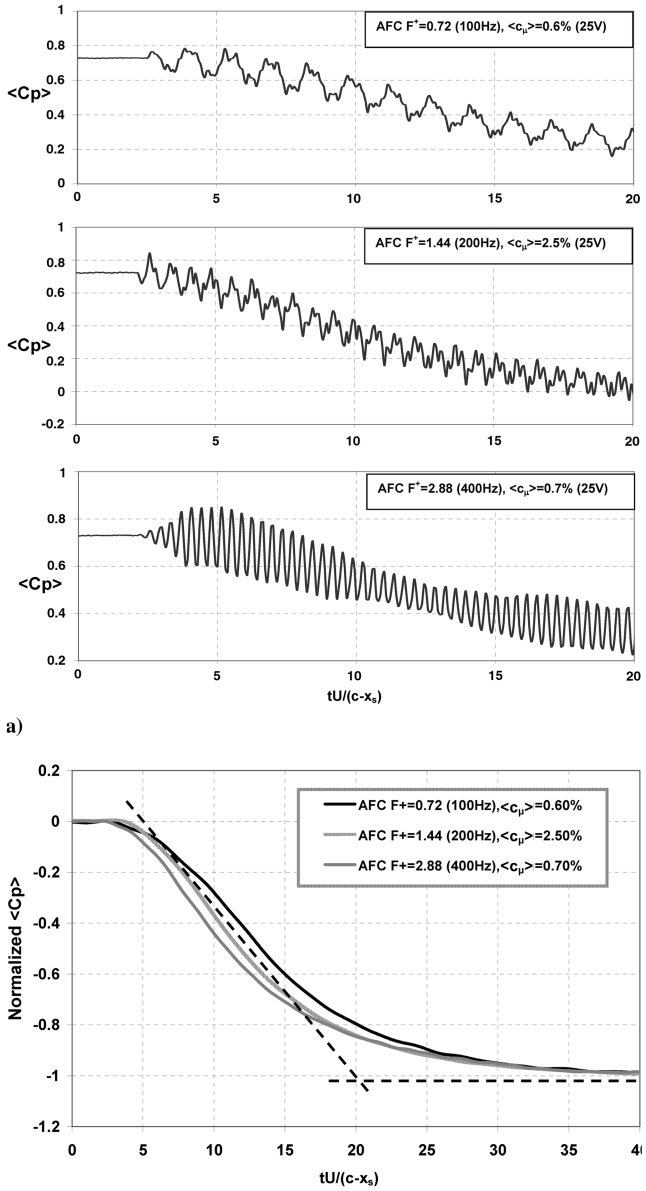

Fig. 10 Pressure signatures on the upper surface, tap $U2$ ($x/c = 0.03$), during the reattachment. $\alpha = 6\,\text{deg}$, clean airfoil, $Re = 2.26 \times 10^5$ (14 m/s). a) phase-averaged C_p coefficient at different frequencies and $\langle C_\mu \rangle$ b) filtered pressure signatures (tap $U2$) at different frequencies and $\langle C_\mu \rangle$.

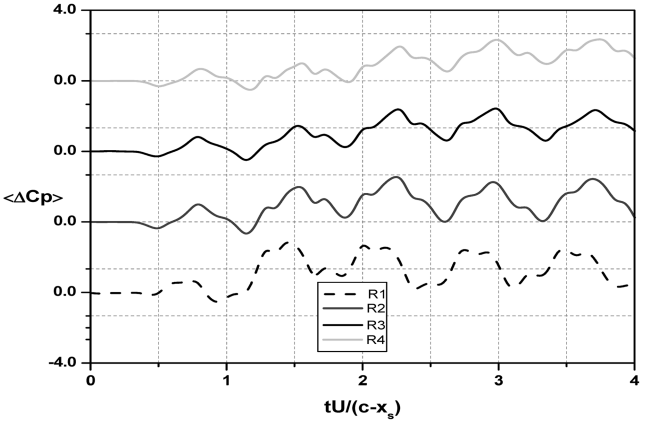

Fig. 11 Pressure signatures on the ramp during the initial stage of reattachment on a clean airfoil at $\alpha = 6\,\text{deg}$, $Re = 2.26 \times 10^5$ (14 m/s), AFC $F^+ = 1.44$ (200 Hz), and $\langle C_\mu \rangle = 2.5\%$.

observed between adjacent transducers, with the sole exception of the delay between the first tap and the rest. This is attributed to the separated region that enabled traveling vortices in the shear layer to transmit pressure fluctuations to a transducer located on the surface from various streamwise locations. This does not happen when the flow is attached, and each passing vortex leaves its footprint on the pressure port located just beneath it.

In contrast, for frequency corresponding to $F^+ = 0.72$, continuous phase differences were detected among all ramp transducers, regardless of tripping (Fig. 12). This could be explained by the fact that a lower excitation frequency generates larger vortices that are reaching the surface, thus trapping fluid between them and sweeping it downstream. This would lead to large pressure fluctuations that propagate downstream at the convection speed of the large vortices. It also seems to be responsible for the slow evolution of time delays between pressure oscillations recorded by taps $R3$ and $R4$ in the case of the clean airfoil (Fig. 12).

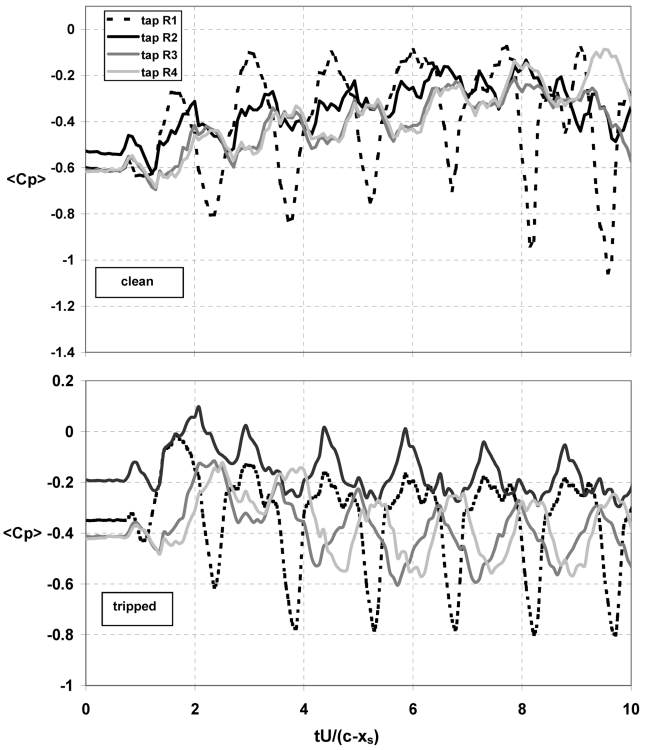

Fig. 12 Pressure signatures on the ramp during the reattachment at $\alpha = 6\,\text{deg}$, $Re = 2.26 \times 10^5$ (14 m/s), AFC $F^+ = 0.72$ (100 Hz), and $\langle C_\mu \rangle = 0.6\%$ (25 V).

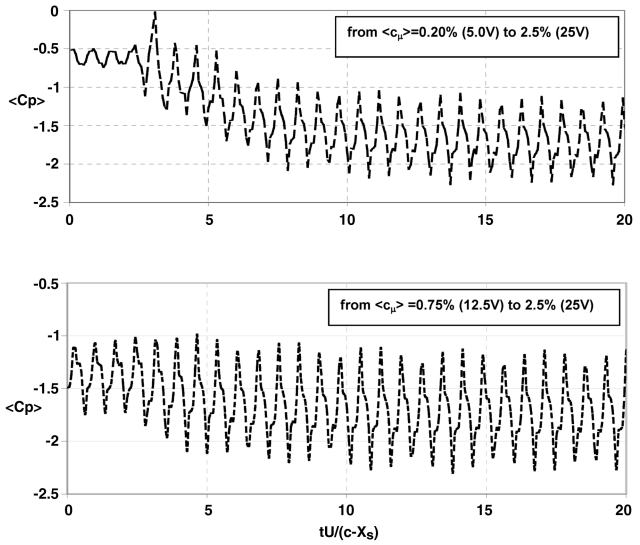

Fig. 13 Pressure signatures on the upper surface during the reattachment at tap $U5$ on a clean airfoil at $\alpha = 6\,\text{deg}$, $Re = 2.26 \times 10^5$ (14 m/s), and AFC $F^+ = 1.44$ (200 Hz).

The reattachment transients on the upper loft of the airfoil for different initial levels of $\langle C_\mu \rangle$ are shown in Fig. 13. The excitation for the two cases shown was at $F^+ = 1.44$, but at different initial $\langle C_\mu \rangle$ values of 0.2 and 0.75%. In each case, the excitation was suddenly increased to $\langle C_\mu \rangle = 2.5\%$, resulting in reattachment. The transient normalized times are almost the same, whereas the initial values of C_p are quite different. It is anticipated that a smooth change of $\langle C_\mu \rangle$ will permit gradual control of the airfoil performance. The force or moment created responds monotonically to the applied $\langle C_\mu \rangle$ and requires a constant time to materialize under the prescribed flight speed and frequency.

B. Controlled Separation Resulting from the Cessation of Actuation

The most obvious way to cause a forced partly attached flow to separate from a surface is an abrupt and complete termination of the excitation. Technically, it is easiest to implement, and from the control point of view, it provides the fundamental open-loop system response. Figure 14 illustrates the pressure transients occurring during separation over the ramp, resulting from the cessation of preexisting actuation at $F^+ = 0.72$, 1.44, and 2.88, respectively. The separation transient time from the ramp's surface is frequency-dependent, in contrast to the reattachment transient that seemed to be frequency-independent, as can also be seen from filtered dynamic pressures (Fig. 14b). The filtering cutoff frequency was chosen to be one-quarter of the initial excitation frequency. If the definition of the termination of the transient remains the same as in the case of the reattachment, then it ends sometime between $11 < \tau < 15$. The process of separation in the region of the ramp is highly nonmonotonic (see Figs. 14a and 14b). For the $F^+ = 0.72$ case, there is a clear time delay in the formation of the lowest-pressure peaks observed by the different taps, suggesting the creation of a dynamic-stall vortex that propagated toward the trailing edge before completing the separation process (see the arrows in Fig. 14a). The transient times on the upstream upper surface and the entire lower surface are about 15–20 (Fig. 15) and they are comparable with the reattachment transient times on these surfaces. Also note the very slow decay of the oscillations at the higher-frequency $F^+ = 2.88$ case that could be the consequence of the cavity and/or actuator resonance (Fig. 14a).

To ensure that cavity and actuator resonances that might have responded to vortex shedding associated with the separated flow do not generate erroneous results, a controlled separation was induced by reducing the excitation amplitude without changing the frequency of the forcing. Tests were carried out in which $\langle C_\mu \rangle$ was reduced from 2.5% to lower various levels at representative frequencies, and

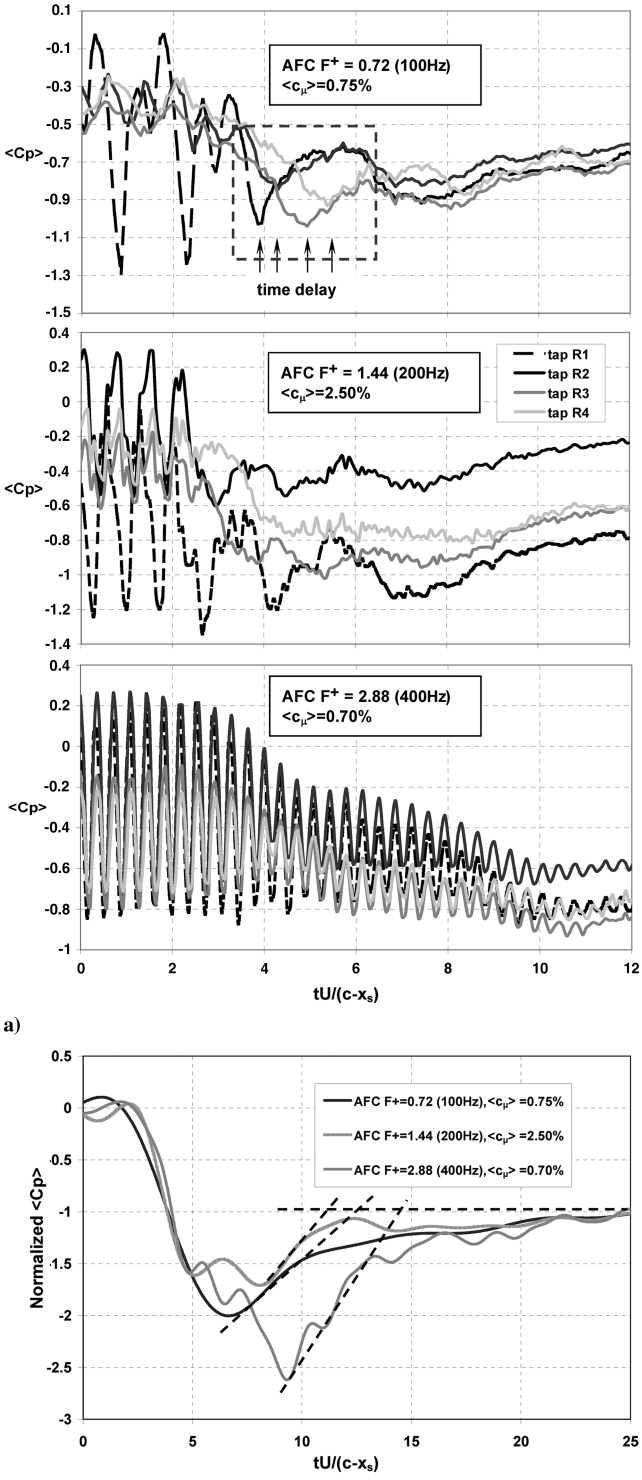

Fig. 14 Pressure signatures on the ramp during the separation from a clean airfoil at $\alpha = 6\,\text{deg}$ and $Re = 2.26 \times 10^5$ (14 m/s): a) phase-averaged C_p coefficient at different frequencies and $\langle C_\mu \rangle$ and b) filtered pressure signatures at tap $R4$ at different frequencies and $\langle C_\mu \rangle$.

they have indicated no change in the transient times recorded. The different values of the final average C_p that was dependent on the final amplitude used indicate that a smooth gradual variation of the wing loading is possible.

VII. Conclusions

Some aspects of the flow around the GLAS II airfoil were experimentally observed. It was shown that the $\langle C_\mu \rangle$ values,

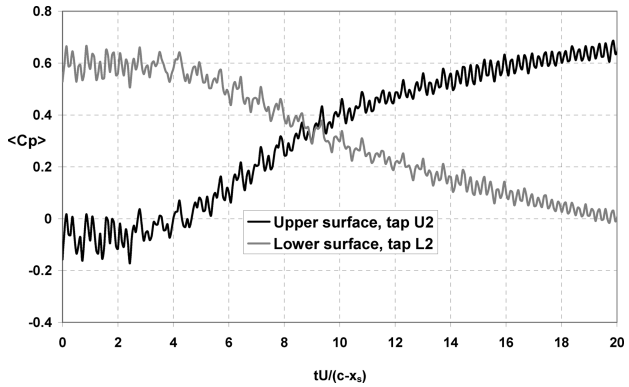

Fig. 15 Pressure signatures on the upper and lower surfaces during the separation from a clean airfoil at $\alpha = 6\,\mathrm{deg}$, $Re = 2.26 \times 10^5$ (14 m/s), AFC $F^+ = 1.44$ (200 Hz), and $\langle C_\mu \rangle = 2.5\%$.

necessary for the reattachment on the concave surface of the GLAS II ramp, are larger by an order of magnitude than the typical values required for reattaching the flow onto a deflected flap of a typical airfoil. Furthermore, the reattachment of the flow to the GLAS II ramp is only partial and it is oscillatory. This difference was explained by the ramp's large concave curvature. Little is known about effect of the curvature on the separation. Stratford [25], who developed empirical criteria for separation, suggested that concavity (i.e., a negative second derivative of the pressure) enhances flow separation, and the same trend possibly holds for periodic excitation. An additional effect of the curvature is related to the centrifugal instability, responsible for the formation of streamwise (Görtler) vortices. The interaction of streamwise and spanwise vortices and their impact on flow control was briefly discussed, as their existence had been demonstrated in the present investigation. The main effect of active flow control on the characteristics of the GLAS II airfoil is the increase in lift resulting from the curvature created by the actuation upstream of the slot. The suction portion of the actuation cycle draws fluid into the slot, accelerating the boundary layer in its vicinity, whereas the blowing portion entrains most of the fluid from upstream and changes the streamline curvature, generating the low-pressure region upstream of the slot.

The transients associated with flow attachment and separation on this airfoil were also studied. The dimensionless transient time $\tau = tU/(c - x_s)$ varied between the values of 15 to 20 over the upper and lower surfaces of the airfoil, but their duration was shorter over the ramp. In addition, τ was frequency-independent of the entire lower surface and on the portion of upper surface upstream of the actuator, but the flow over the ramp depends on the initial frequency of forcing during the transient process of separation.

The possibility of gradual control by introducing smooth changes in $\langle C_\mu \rangle$ was also considered. The transient time in this case is related to the rate of reduction or increase in $\langle C_\mu \rangle$.

The propagation of surface-pressure perturbations after the initialization of the change in excitation occurs at the velocity of sound on the upper surface upstream of the actuation and over the entire lower surface of the airfoil. The slow phase velocity over the ramp is attributed to the passage of the vortices over the pressure sensors and thus scales with the freestream velocity, rather than the velocity of sound. The pressure perturbations exerted by the vortex passage are much larger than the perturbation due to sound. This is the reason for the large phase differences between adjacent pressure sensors located over the ramp. These phase delays are absent elsewhere over the airfoil. In some instances, bubbles associated with the partial separation affect more than one pressure sensor simultaneously, thus changing or even eliminating phase delay.

Acknowledgments

The experiment was partially supported by a NASA Research Announcement (NRA) under grant NNX07AB73A#1. The authors are grateful to Lutz Taubert and Benjamin Wesley for their help in performing the experiments.

References

[1] Greenblatt, D., and Wygnanski, I., "Control of Separation by Periodic Excitation," *Progress in Aerospace Sciences*, Vol. 36, No. 7, 2000, pp. 487–545. doi:10.1016/S0376-0421(00)00008-7

[2] Scott Collis, S., Joslin, R. D., Seifert, A., and Theofilis, V., "Issues in Active Flow Control: Theory, Control, Simulation and Experiment," *Progress in Aerospace Sciences*, Vol. 40, No. 4, 2004, pp. 237–289. doi:10.1016/j.paerosci.2004.06.001

[3] Schmalzel, M., Varghese, P., and Wygnanski, I., "Steady and Oscillatory Flow Control Tests for Tilt Rotor Aircraft," *Active Flow Control*, Numerical Fluid Mechanics and Multidisciplinary Design, Vol. 95, Springer, Berlin, 2007, pp. 190–211.

[4] Lachmann, G.V. ed., *Boundary Layer and Flow Control: Its Principles and Application*, Pergamon, New York, 1961.

[5] Cerchie, D., Halfon, E., Hammerich, A., Han, G., Taubert, L., Trouve, L., Varghese, P., and Wygnanski, I., "Some Circulation and Separation Control Experiments," *Application of Circulation Control Technologies*, edited by R. D. Joslin, and G. S. Jones, Progress in Astronautics and Aeronautics, Vol. 214, AIAA, Reston, VA, 2006.

[6] Nishri, B., and Wygnanski, I., "Effects of Periodic Excitation on Turbulent Flow Separation from a Flap," *AIAA Journal*, Vol. 36, No. 4, 1998, pp. 547–556. doi:10.2514/2.428

[7] Darabi, A., and Wygnanski, I., "Active Management of Naturally Separated Flow over a Solid Surface. Part 1: The Forced Reattachment Process," *Journal of Fluid Mechanics*, Vol. 510, July 2004, pp. 105–129. doi:10.1017/S0022112004009231

[8] Darabi, A., and Wygnanski, I., "Active Management of Naturally Separated Flow over a Solid Surface. Part 2: The Separation Process," *Journal of Fluid Mechanics*, Vol. 510, July 2004, pp. 131–144. doi:10.1017/S0022112004009243

[9] Kit, E., Wygnanski, I., Friedman, D., Krivonosova, O., and Zhilenko, D., "On the Periodically Excited, Plane Turbulent Mixing Layer, Emanating from a Jagged Partition," *Journal of Fluid Mechanics*, Vol. 589, Oct. 2007, pp. 479–507. doi:10.1017/S0022112007007884

[10] Neuendorf, R., Lourenco, L., and Wygnanski, I., "On Large Streamwise Structures in a Wall Jet Flowing over a Circular Cylinder," *Physics of Fluids*, Vol. 16, No. 7, 2004, pp. 2158–2169. doi:10.1063/1.1703531

[11] Han, G., de Zhou, M., and Wygnanski, I., "On Streamwise Vortices and Their Role in the Development of a Curved Wall Jet," *Physics of Fluids*, Vol. 18, No. 9, 2006, pp. 095104-1–095104-14. doi:10.1063/1.2353403

[12] Neuendorf, R., "Turbulent Wall Jet Along a Convex Curved Surface," Ph.D. Thesis, Technical Univ. of Berlin, Berlin, and Mensch & Buch Verlag, Berlin, 2000.

[13] Greenblatt, D., Paschal, Yao, C., Harris, J. K., Schaeffler, N., and Washburn, A., "Experimental Investigation of Separation Control Part 1: Baseline and Steady Suction," *AIAA Journal*, Vol. 44, No. 12, Dec. 2006, pp. 2820–2830. doi:10.2514/1.13817

[14] Greenblatt, D., Paschal, K. B., Yao, C.-S., and Harris, J., "Experimental Investigation of Separation Control Part 2: Zero Mass-Flux Oscillatory Blowing," *AIAA Journal*, Vol. 44, No. 12, Dec. 2006, pp. 2831–2845. doi:10.2514/1.19324

[15] Glauert, M. B., "The Application of the Exact Methods of Airfoil Design," Aeronautical Research Council Reports and Memoranda No. 2683, London, 1955.

[16] Glauert, M. B., Walker, W. S., Raymer, W. G., and Gregory, N., "Wind Tunnel Tests on Thick Suction Airfoil with a Single Slot," Aeronautical Research Council Reports and Memoranda No. 2646, London, Oct. 1948.

[17] Salter, C., Miles, C. J. W., and Owen, R., "Test on GLAS II Wing without Suction in the Compressed Wind Tunnel," Aeronautical Research Council Reports and Memoranda No. 2540, London, 1948.

[18] Gregory, N., and Walker, W. S., "Further Wind Tunnel tests on a 30% Symmetrical Suction Airfoil with a movable Flap," Aeronautical Research Council Reports and Memoranda No. 287, London, 1950.

[19] Thwaites, B. ed., *Incompressible Aerodynamics, An Account of the Theory and Observation of the Steady Flow of Incompressible Fluid*

Past Airfoils, Wings and Other Bodies, Dover, New York, 1960, pp. 245–248.

[20] Wygnanski, I., "On Active Control of Separation from Bluff Bodies," *International Conference on Jets, Wakes and Separated Flows (ICJWSF-2005)* [CD-ROM], Japan Society of Mechanical Engineering, Tokyo, Oct. 2005, Paper P-IL4.

[21] Rumsey, C., Sanetrik, M., Biedron, R., Melson, N. D., and Parlette, E., "Efficiency and Accuracy of Time-Accurate Turbulent Navier-Stokes Computations," *Computers and Fluids*, Vol. 25, No. 2, pp. 217–236, 1996, pp. 217–236. doi:10.1016/0045-7930(95)00043-7

[22] Wesley, B. F., Zakharin, B., and Wygnanski, I., "Effects of Flow Control on Modified GLAS II Airfoil,"*Journal of Aircraft* (to be published).

[23] Saric, W. S., "Gortler Vortices," *Annual Review of Fluid Mechanics*, Vol. 26, 1994, pp. 379–409. doi:10.1146/annurev.fl.26.010194.002115

[24] Seifert, A., Bachar, T., Koss, D., Shepshelovich, M., and Wygnanski, I., "Oscillatory Blowing: A Tool to Delay Boundary-Layer Separation," *AIAA Journal*, Vol. 31, No. 11, 1993, pp. 2052–2060. doi:10.2514/3.49121

[25] Stratford, B. S., "The Prediction of the Separation of the Turbulent Boundary Layer," *Journal of Fluid Mechanics*, Vol. 5, No. 1, 1959, pp. 1–16. doi:10.1017/S0022112059000015